HHS Public Access

Author manuscript

J AAPOS. Author manuscript; available in PMC 2017 August 01.

Published in final edited form as:

J AAPOS. 2016 August ; 20(4): 343–347. doi:10.1016/j.jaapos.2016.05.015.

Isolated schwannoma involving extraocular muscles

Fatma Yulek, MD[a] and **Joseph L. Demer, MD, PhD**[a,b]

[a]Department of Ophthalmology, Stein Eye Institute, UCLA, Los Angeles, California

[b]Department of Neurology, Neuroscience Interdepartmental Program, Bioengineering Interdepartmental Program, UCLA, Los Angeles, California

Abstract

Background—Progressive strabismus initially considered idiopathic may be caused by isolated schwannomas of motor nerves to extraocular muscles, detectable only on careful imaging. This study reviewed clinical experience of a referral practice in identifying schwannomas on magnetic resonance imaging (MRI).

Methods—We reviewed 647 cases imaged for strabismus to identify presumed cranial nerve schwannomas, identified by gadodiamide-enhanced, high-resolution surface coil orbital MRI and thin-section cranial MRI. Clinical features and management were correlated with MRI.

Results—Schwannomas were identified as fusiform intraneural enlargements in 8 cases: 1 affecting the trochlear nerve; 2, the abducens nerve; and 5 the oculomotor nerve. Involved muscles were atrophic. Both abducens schwannomas, 1 superior oblique, and 1 oculomotor schwannoma were subarachnoid; 3 were intraorbital, and bilateral oculomotor lesions of 1 case extended from cavernous sinus to orbit. Associated strabismus progressed for 3-17 years. Abducens schwannoma caused esotropia; trochlear schwannoma caused hypertropia and cyclotropia. Intracranial oculomotor schwannoma caused mydriasis and exotropia. Intraorbital schwannoma caused exotropia with or without hypertropia. Since lesion diameters were 3–9 mm, 6 had been previously missed on routine MRI.

Conclusions—Progressive, acquired strabismus may be caused by isolated cranial nerve schwannomas, representing about 1% of strabismus cases in this study, involving the oculomotor more than abducens nerve. Because most schwannomas are small and deep in the orbit, findings could be readily missed by routine imaging, leading to a possible diagnosis of idiopathic strabismus. Schwannomas should be suspected when extraocular muscles are atrophic, but the causative lesions themselves are identifiable only using targeted, high resolution MRI.

Correspondence: Joseph L. Demer, MD, PhD, Stein Eye Institute, University of California, Los Angeles, 100 Stein Plaza, Los Angeles, CA, 90095-7002 (jld@jsei.ucla.edu).

FDA disclosure: Investigational surface coils were used in MRI imaging.

Presented at the 42nd Annual Meeting of the American Association for Pediatric Ophthalmology and Strabismus, Vancouver, British Columbia, April 6-10, 2016.

Progressive acquired strabismus frequently presents a diagnostic dilemma for clinicians. Etiologies such as myasthenia gravis, thyroid orbitopathy, and ischemic cranial neuropathy may be readily diagnosed on clinical grounds by physical examination and specific laboratory tests.[1-3] Other cases of progressive acquired strabismus are often simply categorized as “idiopathic” without efforts for identification of etiology. Improvements in imaging techniques have made it possible for clinicians to diagnose underlying causes in these “idiopathic” cases.[4] Isolated schwannomas of cranial motor nerves are among these underdiagnosed cases.[5] These well-defined, slowly progressive tumors, that originate from Schwann cells of peripheral nerves, derange ocular motility in several ways. Typically the clinical course of schwannomas is that of progressive cranial nerve dysfunction or relative stability.[6] However, the clinical picture is seldom as clear as with complete cranial nerve palsy. Partial cranial nerve palsies create atypical strabismus presentations that can be easily misdiagnoed. This study employed targeted high-resolution magnetic resonance imaging (MRI) to provide insight into the imaging and clinical properties in cases of progressive acquired strabismus caused by schwannomas.

Subjects and Methods

This is retrospective analysis of data collected in an ongoing, prospective study of strabismus that has been conducted continuously since 1990 at the Jules Stein (now the Stein) Eye Institute, UCLA. At time of analysis in late 2015, a total of 647 patients had undergone high-resolution orbital MRI for strabismus. Among these were 36 cases of oculomotor nerve palsy, 95 cases of trochlear nerve palsy, and 32 cases of abducens nerve palsy. A nonconsecutive subset of these patients who had progressive, acquired cranial neuropathy suspicious for cranial nerve involvement also underwent MRI of the intracranial space. Schwannoma was diagnosed by clinical course and typical radiological properties. Written informed consent was obtained prospectively according to a protocol approved by the UCLA Human Subject Protection Committee, later renamed the UCLA Medical I Review Board for the Protection of Human Subjects, from patients who were recruited from referral strabismus practices. Complete ophthalmologic examination and ocular motility evaluation, including prism cover testing, photography, and Hess screen testing, was performed for appropriate patients.

A 1.5 T General Electric Signa scanner (Milwaukee, WI) was used in orbital imaging, as previously described.[7] Imaging was performed using an array of surface coils embedded in a transparent facemask (Medical Advances, Milwaukee, WI) for improved resolution and another array of individually illuminated fixation targets to avoid eye motion artifacts. The standard head coil was used for imaging at and posterior to the orbital apex in some subjects at 1.5 or 3 T. When surface coils were used, quasicoronal images perpendicular to the long axis of orbit and quasisagittal images parallel to the long axis of the orbit were obtained at 2 mm thickness in a matrix of 256 × 256 over a field view of 6–8 cm for a resolution in plane of 234–312 μm, respectively. Brainstem imaging was performed in 0.8 mm thickness planes using the heavily T2-weighted FIESTA sequence to obtain contrast of cranial nerves against the subarachnoid cerebrospinal fluid. Resolution in the brainstem region was 195 μm in a 512 × 512 matrix over a 10 cm field of view with 10 excitations.

Results

A total of 8 cases (3 of which were previously presented in brief reports[7,8]) were identified that represent a spectrum of clinical forms of isolated cranial nerve schwannomas. Their clinical and imaging properties are summarized in Table 1. Clinical summaries are provided for informative cases not previously described.

Oculomotor Schwannomas

The oculomotor nerve was involved in 5 cases. One case had bilateral neuromas extending from the cavernous sinus to the orbit. One case was located in the subarachnoid space, and 3 cases were located entirely in the deep orbit. All cases had unilateral schwannomas except the patient who had bilateral schwannomas (case 4) extending from the cavernous sinus to the orbit.

Intra-orbital Oculomotor Schwannomas

Case 1, with intraorbital neuroma of the medial rectus motor nerve, was a 60-year-old man who had a 10-year history of occasional horizontal, binocular diplopia with progressive right medial rectus paresis. He had 50^{Δ} right exotropia at distance and 35^{Δ} at near, with limited adduction and slow adduction saccades of the right eye. Cranial nerves and ocular motility were otherwise normal. Orbital MRI disclosed medial rectus muscle atrophy (Figure 1) and a 2.9 × 3.9 mm contrast-enhancing tumor in the motor nerve to the medial rectus, deep in the orbit and close to the muscle (Figure 2).

In case 2, a 21-year-old woman complaining of diplopia, the schwannoma was located deep in the orbit. She had noticed slowly progressive right exotropia since giving birth 3 years previously. Routine brain MRI was interpreted as normal. Cranial nerves were clinically normal except that the right eye could not adduct more than about 20° to the right of midline, with profound slowing of the adduction saccade. Right exotropia exceeded 100^{Δ}, with 30^{Δ} right hypertropia. Ophthalmoscopy using a quantitative technique for fundus torsion demonstrated 30° right fundus excycloposition and 25° left excycloposition.[9] Routine MRI revealed no lesion along the subarachnoid oculomotor nerve, no evidence of infarction in the midbrain, or any lesion in apical orbital portion of inferior division of the oculomotor nerve. High-resolution surface coil MRI of the orbits demonstrated profound atrophy of the deep portion of the right medial rectus muscle (Figure 3) and a small enhancing lesion (3.3 × 2.8 mm) in the path of the intraorbital motor nerve to the right medial rectus muscle (Figure 4) compatible with schwannoma. The medial rectus muscle atrophy corresponded to the location of the schwannoma (Figure 3). All other extraocular muscles exhibited normal size, and all extraocular muscles had normal paths.

Clinical details of case 3 have been published previously.[7]

Subarachnoid Oculomotor Schwannomas

Case 4 was a 60-year-old man complaining of binocular oblique diplopia that was progressively worsening for 17 years. He had right exotropia and hypertropia, and bilateral subarachnoid oculomotor nerve schwannomas. In the coronal plane the schwannomas

measured 7.5 × 10 mm on the right and 2.6 × 7.7 mm on the left, extending from cavernous sinus to each orbit with bright signals in T2 images (Figure 5). Atrophy of muscles innervated by the involved oculomotor nerves was pronounced, but muscles innervated by other cranial nerves were normal. These large bilateral tumors were easily diagnosed in initial routine imaging in a patient presenting with obvious clinical signs of oculomotor nerve involvement and progressive clinical course with striking atrophy of involved muscles.

Case 5 was a 55-year-old woman who experienced oblique and tilted binocular diplopia for 5 years. She exhibited left mydriasis, 45^{Δ} distance exotropia increasing in dextroversion, left hypertropia in supraversion, and right hypertropia in infraversion with 5° right incyclotropia as measured by quantitative ophthalmoscopy. High-resolution orbital MRI demonstrated reduction in size of the intraorbital motor branches of the right oculomotor nerve, with atrophy of the associated extraocular muscles. Thin section axial oblique MRI of the skull base disclosed a contrast-enhancing tumor of the right interpeduncular oculomotor nerve approximately 5 mm in diameter at the crossing point of the postcommunicating artery, as previously published.[7] An magnetic resonance angiogram showed no abnormal vascularity.

Abducens Schwannomas

Two abducens schwannomas (cases 6 and 7) were located in the subarachnoid space. Both cases had abducens paresis and esotropia with progressive clinical course without involvement of other cranial nerves. A relatively large tumor, measuring 6 × 12 mm in case 7 was easily diagnosed (Figure 6). Case 7 exhibited atrophy of the left lateral rectus muscle. Case 6, with a schwannoma measuring 5 mm in diameter, had compartmental abducens nerve palsy, as previously described,[8] showing atrophy of the superior half of the lateral rectus muscle with sparing of the inferior half due to preserved inferior compartmental innervation.

Trochlear Schwannoma

Case 8 was a 55-year-old man with a 5-year history of progressively worsening vertical torsional binocular diplopia, without associated history of trauma or neurological disease. He adopted a compensatory right head tilt. Multipositional surface coil MRI of the orbits showed intact lateral rectus–superior rectus band ligaments in both eyes but anisotropic atrophy of the left superior oblique (Figure 7), with marked attenuation of contractility in infraduction. Anisotropic atrophy of the superior oblique muscle, typified by elongated superior oblique cross section, was due to greater atrophy in one compartment than the other.[10] No other orbital abnormalities were apparent. Brain MRI at 3T with and without contrast revealed a 5 mm enhancing nodule in the left ambient cistern (Figure 8) lying along the expected course of the left trochlear nerve. No acute intracranial mass effect, hemorrhage, hydrocephalus, or midline shift was observed.

Discussion

The important common findings in all patients with schwannomas involving the extraocular muscles were progressive clinical course, atrophy of involved muscles, highly selective involvement of cranial nerves, and nodular or fusiform hyperintense neural lesions in on T2

- weighted and contrast-enhanced T1-weighted MRI. The clinical features of these patients vary according to the nerve involved as well as size and location of the tumor such that schwannoma as underlying etiology is nonobvious. As evident in this series, involvement of the intraorbital branches of the oculomotor nerve may present with progressive exotropia that can easily be mistaken for decompensation of nonparalytic intermittent exotropia.

Lesions involving the more proximal oculomotor nerve, on the other hand, presented variable pictures according to the involved motor branches. Ptosis and pupil abnormalities were present, with subarachnoid and cavernous oculomotor nerve lesions. Intraorbital oculomotor schwannomas mostly involved the medial rectus muscle motor \. All of these lesions were missed on routine imaging. There may be several causes for this diagnostic failure. First, only progressive exotropia with isolated medial rectus paresis and without involvement of other muscles innervated by the oculomotor nerve may not seem suggestive of a neuroma. Second, the small lesion located deep in the orbit is almost impossible to detect by routine MRI with a head coil. Third, the rarity of these neuromas may be a factor.

Schwannomas are usually presumptively diagnosed by MRI findings because their appearance on these images is considered pathognomonic and because tumor resection for histopathological confirmation is seldom clinically necessitated by mass effect but is certain to sacrifice any residual function of the involved cranial nerve. In all our patients atrophy of muscles in orbital MRI innervated by the motor nerve branch was an important clue to the presence of these lesions. If this clue is recognized, careful high-resolution MRI can reveal these lesions. Compartmental atrophy of the lateral rectus muscle in coronal images may suggest abducens schwannoma.[8,11,12]

Although various presentations have been described,[13] the classical appearance of orbital schwannoma on MRI is usually described as a lesion with low signal on T1-weighted images and a high signal on T2-weighted images that can be homogeneously or heterogeneously enhanced by intravenous contrast. All cases in the current series were nodular or fusiform hyperintense lesions in T2 and contrast T1 images.

Many lesions presenting as round or ovoid masses in the orbit should be differentiated from schwannoma. These include cavernous hemangioma, pleomorphic adenoma of the lacrimal gland, dermoid cyst, and solitary fibrous tumor of the orbit (a spindle cell neoplasm arising from mesenchymal structures). MRI can readily distinguish some of these tumors on the basis of characteristic findings.[14-16] Cavernous hemangioma, for example, is characterized by “progressive enhancement over time,”[16] whereas pleomorphic adenoma is generally centered in the lacrimal gland and is well-circumscribed and T2 hyperintense.[17] A dermoid cyst characteristically has T1 hyperintensity and lacks of enhancement on MRI. On the other hand, precontrast MRI findings and an enhancement pattern of solitary fibrous tumor in the orbit may resemble those of schwannoma.[18]

The degree of enhancement on T2-weighted imaging in orbital solitary fibrous tumor is marked and uniform, whereas in schwannoma the areas generally show no enhancement.[19] This different enhancement pattern in areas of very high signal intensity in the tumors might be helpful in the differential diagnosis, as is their highly specific localization along cranial

nerves. Moreover, schwannomas typically produce extraocular muscle dysfunction when much smaller than other lesions that may be considered in the differential diagnosis. The clinical picture and routine imaging may be misleading in strabismus cases due to schwannomas that are therefore considered idiopathic.

Lack of a definite diagnosis can lead to considerable anxiety for patients and repeated rounds of costly evaluation for other causes of strabismus, such as myasthenia gravis, paraneoplastic syndromes, and demyelination. In progressive cases with cranial nerve involvement, diagnosis can be revealed only with careful evaluation of targeted, high-resolution MRI.

Acknowledgments

Grant support: U.S. Public Health Service grant EY008313 and an Unrestricted Grant from Research to Prevent Blindness. J. Demer holds the Arthur Rosenbaum Chair of Pediatric Ophthalmology.

References

1. Gilbert J, Dailey RA, Christensen LE. Characteristics and outcomes of strabismus surgery after orbital decompression for thyroid eye disease. J AAPOS. 2005; 9:26–30. [PubMed: 15729277]
2. Rowe F, UK VISg. The profile of strabismus in stroke survivors. Eye (Lond). 2010; 24:682–5. [PubMed: 19521433]
3. Peragallo JH, Velez FG, Demer JL, Pineles SL. Long-term follow-up of strabismus surgery for patients with ocular myasthenia gravis. J Neuroophthalmol. 2013; 33:40–44. [PubMed: 23403387]
4. Demer JL. Muscle paths matter in strabismus associated with axial high myopia. Am J Ophthalmol. 2010; 149:184–6.e1. [PubMed: 20103050]
5. Ohata K, Takami T, Goto T, Ishibashi K. Schwannoma of the oculomotor nerve. Neurol India. 2006; 54:437–9. [PubMed: 17114862]
6. Elmalem VI, Younge BR, Biousse V, et al. Clinical course and prognosis of trochlear nerve schwannomas. Ophthalmology. 2009; 116:2011–16. [PubMed: 19699532]
7. Demer JL, Ortube MC, Engle EC, Thacker N. High-resolution magnetic resonance imaging demonstrates abnormalities of motor nerves and extraocular muscles in patients with neuropathic strabismus. J AAPOS. 2006; 10:135–42. [PubMed: 16678748]
8. Clark RA, Demer JL. Lateral rectus superior compartment palsy. Am J Ophthalmol. 2014; 157:479–487.e2. [PubMed: 24315033]
9. Kothari MT, Venkatesan G, Shah JP, Kothari K, Nirmalan PK. Can ocular torsion be measured using the slitlamp biomicroscope? Indian J Ophthalmol. 2005; 53:43–7. [PubMed: 15829746]
10. Shin SY, Demer JL. Superior oblique extraocular muscle shape in superior oblique palsy. Am J Ophthalmol. 2015; 159:1169–79.e2. [PubMed: 25747676]
11. Demer JL. Compartmentalization of extraocular muscle function. Eye (Lond). 2015; 29:157–62. [PubMed: 25341434]
12. Le A, Poukens V, Ying H, Rootman D, Goldberg RA, Demer JL. Compartmental innervation of the superior oblique muscle in mammals. Invest Ophthalmol Vis Sci. 2015; 56:6237–46. [PubMed: 26426404]
13. Wang Y, Xiao LH. Orbital schwannomas: findings from magnetic resonance imaging in 62 cases. Eye (Lond). 2008; 22:1034–9. [PubMed: 17464300]
14. Goh PS, Gi MT, Charlton A, et al. Review of orbital imaging. Eur J Radiol. 2008; 66:387–95. [PubMed: 18501542]
15. Lemke AJ, Kazi I, Felix R. Magnetic resonance imaging of orbital tumors. Eur Radiol. 2006; 16:2207–19. [PubMed: 16583212]

16. Xian J, Zhang Z, Wang Z, et al. Evaluation of MR imaging findings differentiating cavernous haemangiomas from schwannomas in the orbit. Eur Radiol. 2010; 20:2221–8. [PubMed: 20393718]
17. Mafee MF, Edward DP, Koeller KK, Dorodi S. Lacrimal gland tumors and simulating lesions. Clinicopathologic and MR imaging features. Radiol Clin North Am. 1999; 37:219–39. xii. [PubMed: 10026740]
18. Savino G, Aliberti S, Colucci D, Perrotta V, Balestrazzi E. Atypical presentation of a case of solitary fibrous tumor of the orbit. Orbit. 2009; 28:176–8. [PubMed: 19839906]
19. Zhang Z, Shi J, Guo J, Yan F, Fu L, Xian J. Value of MR imaging in differentiation between solitary fibrous tumor and schwannoma in the orbit. AJNR Am J Neuroradiol. 2013; 34:1067–71. [PubMed: 23306015]

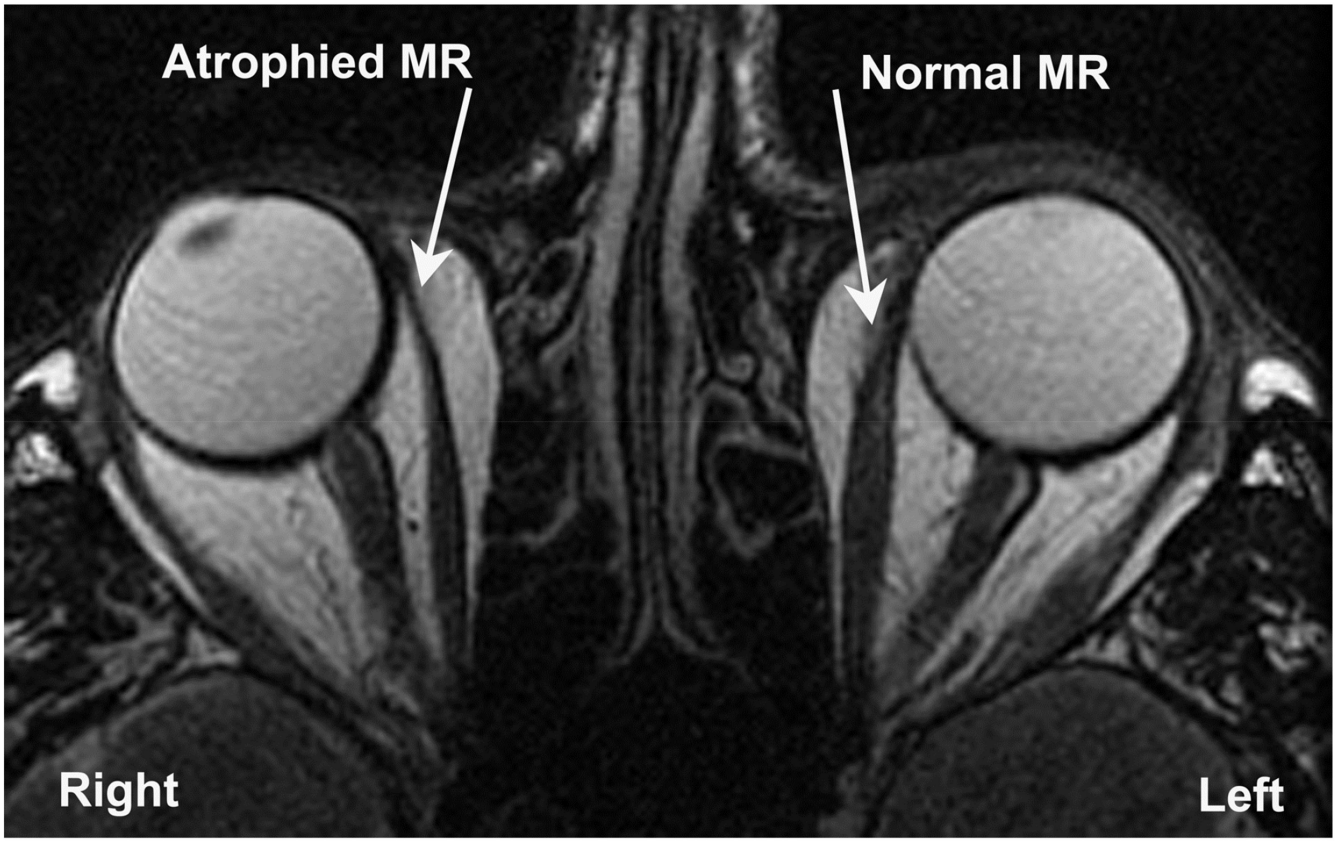

FIG 1.
Axial T2-weighted surface coil MRI disclosing right medial rectus muscle (*MR*) atrophy in case 1.

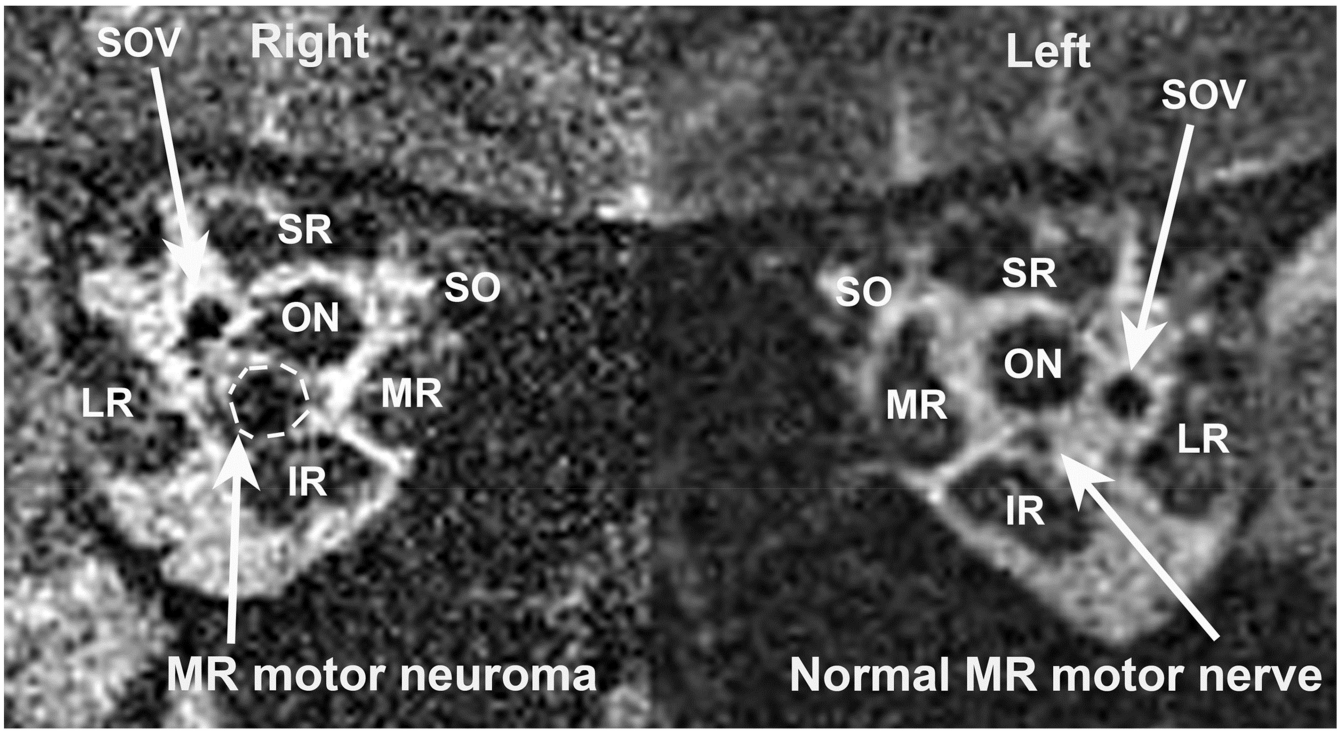

FIG 2.

T2 surface coil MRI in case 1 demonstrating tumor in the motor nerve to the medial rectus muscle (*MR*) measuring 2.9 × 3.9 mm. *IR*, inferior rectus muscle; *LR*, lateral rectus muscle; *ON*, optic nerve; *SO*, superior oblique muscle; *SOV*, superior ophthalmic vein; *SR*, superior rectus muscle.

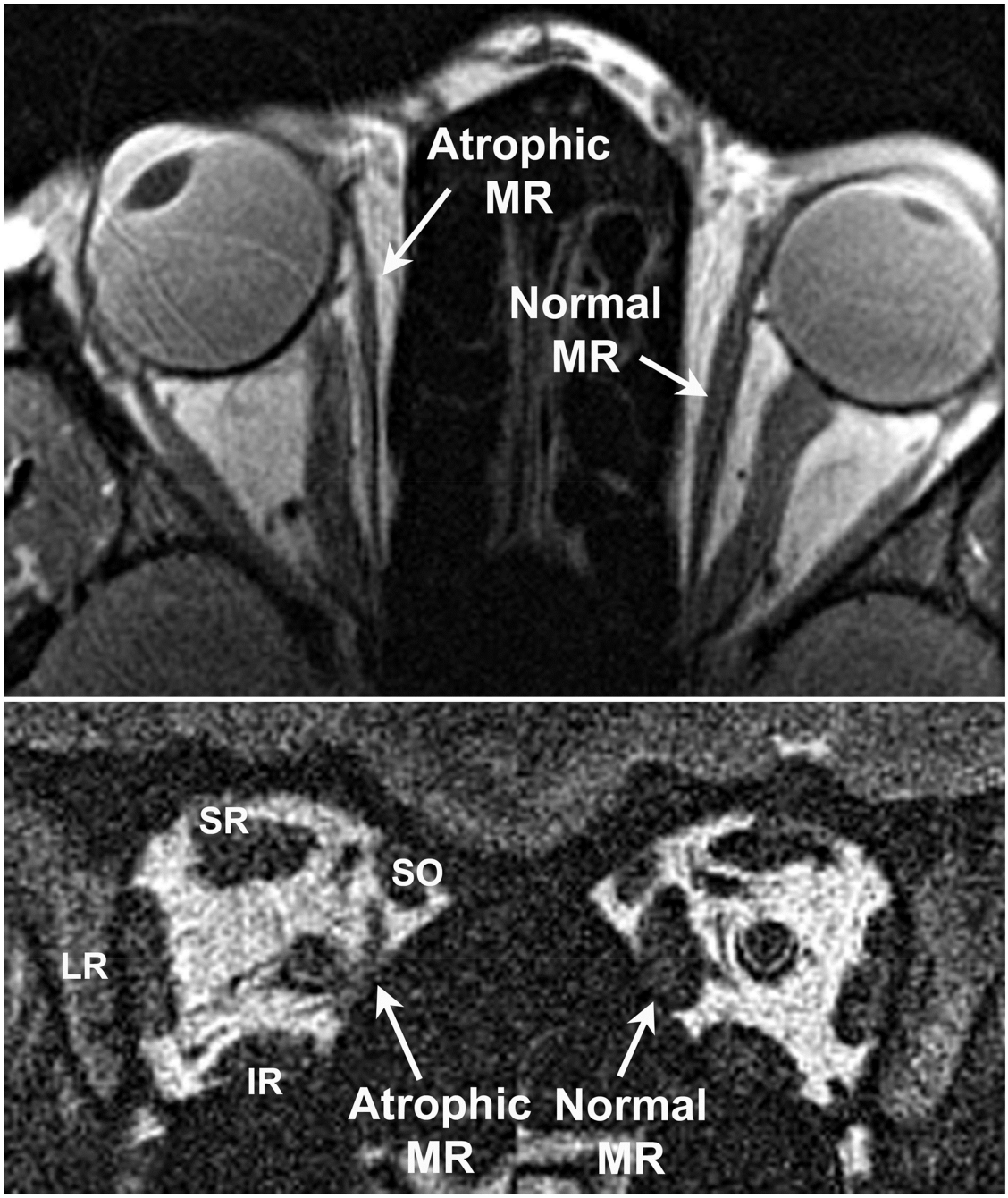

FIG 3.

High-resolution surface coil MRI of the orbits of case 2 with right medial rectus motor nerve schwannoma demonstrating profound atrophy of the deep portion of the right medial rectus muscle (MR).

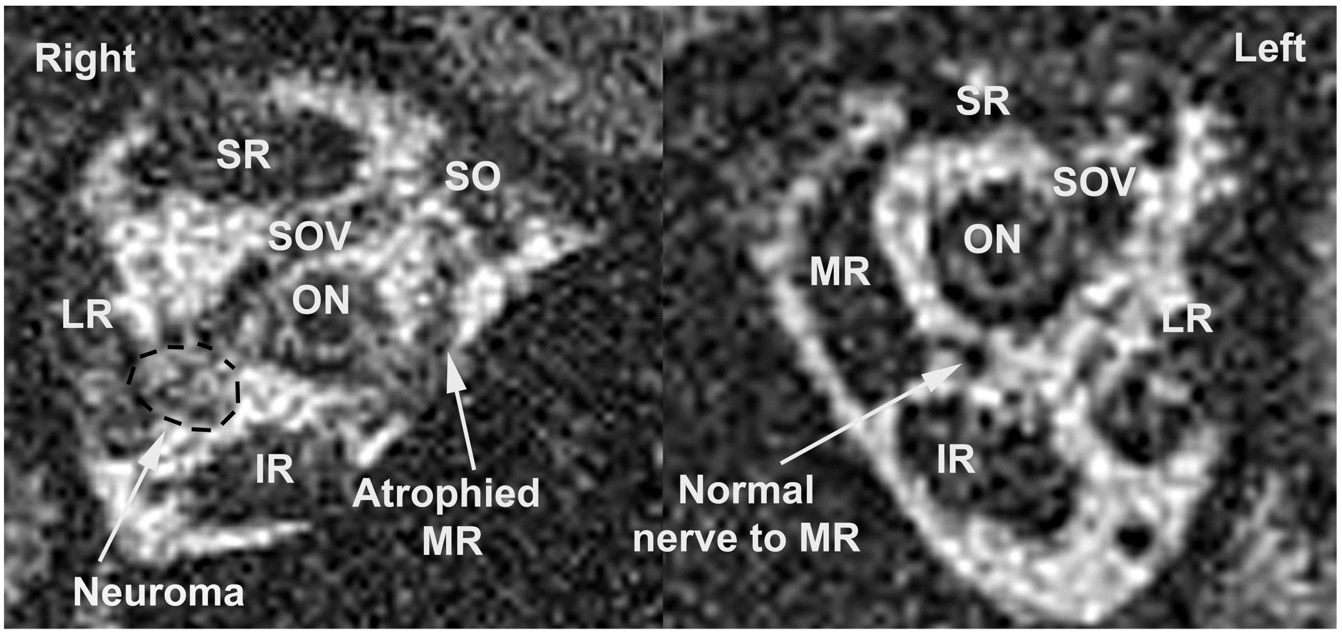

FIG 4.

Contrast-enhanced coronal T1-weighted surface coil MRI of right orbit of case 2 demonstrating a 3.3×2.8 mm enhancing lesion in the path of the motor nerve to the medial rectus muscle compatible with schwannoma. *IR*, inferior rectus muscle; *LR*, lateral rectus muscle; *MR*, medial rectus muscle; *ON*, optic nerve; *SOV*, superior ophthalmic vein; *SR*, superior rectus muscle.

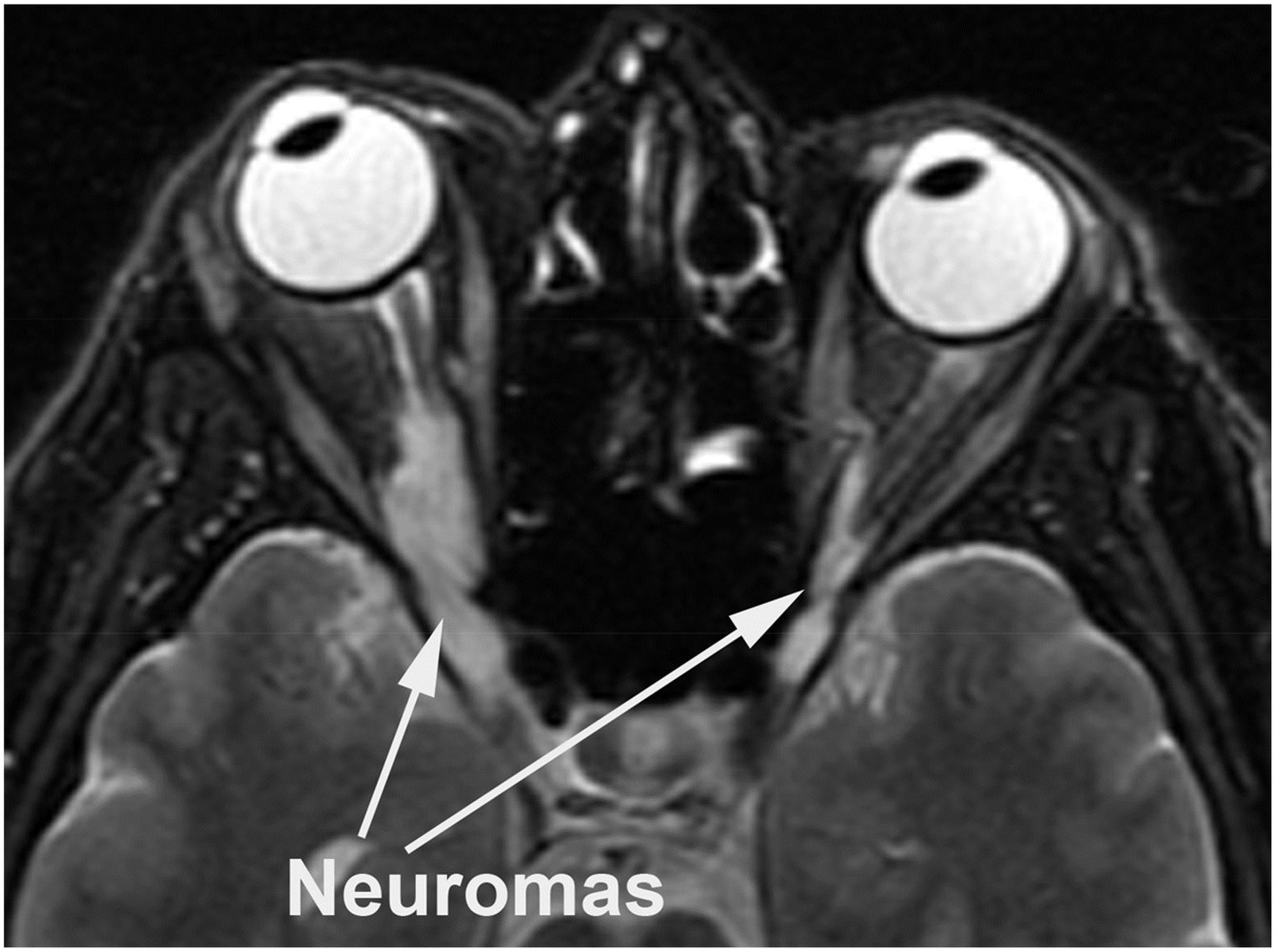

FIG 5.

Axial T2 weighted MRI of brain of case 4 demonstrating subarachnoid and cavernous sinus schwannomas measuring 7.5×10.0 mm on the right and 2.6×7.7 mm on the left extending into each orbit. Note the bright T2 signals in the tumors.

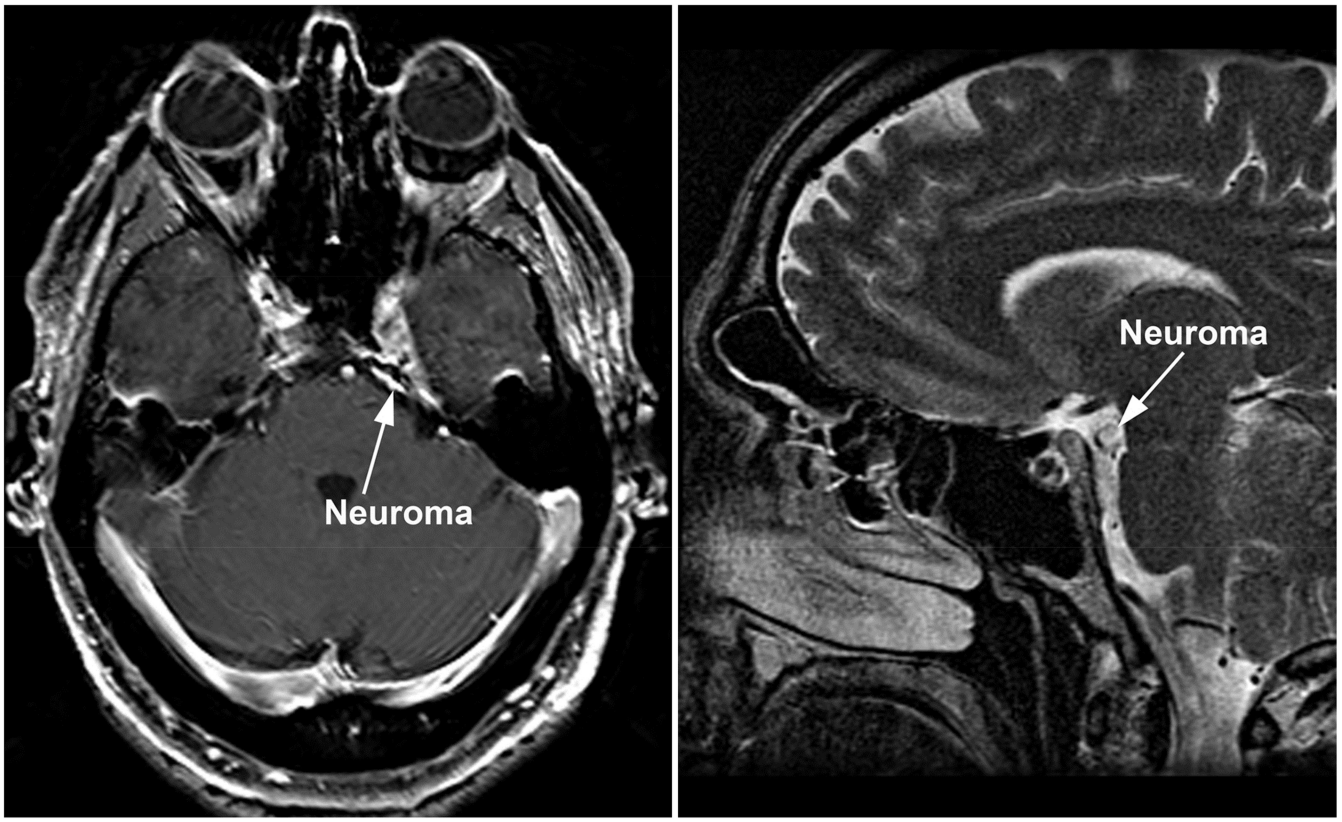

FIG 6.
Gadolinium enhanced, axial T1 MRI demonstrating a large, enhancing neuroma of Case 7 located in left cavernous sinus and subarachnoid space.

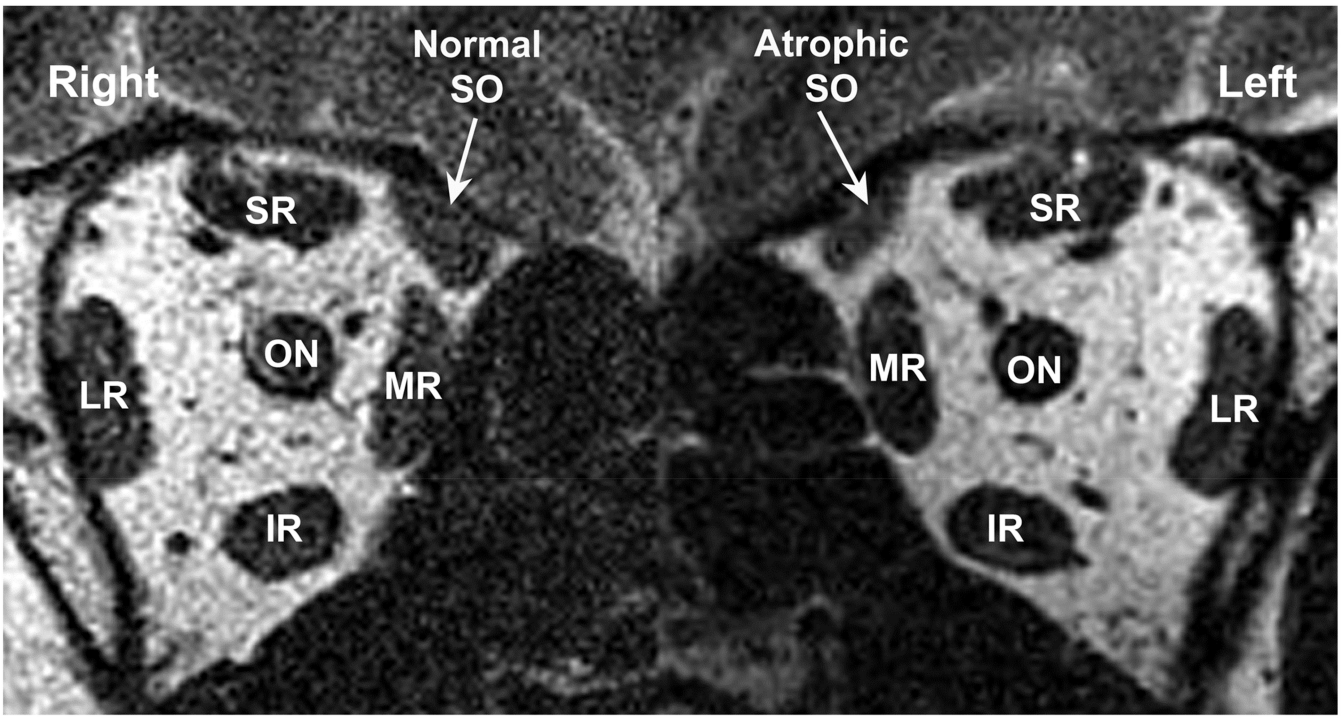

FIG 7.

Surface coil MRI demonstrating anisotropic atrophy of the left superior oblique muscle (*SO*) in Case 8. *IR*, inferior rectus muscle; *LR*, lateral rectus muscle; *MR*, medial rectus muscle; *ON*, optic nerve; *SR*, superior rectus muscle. The atrophy thins the minor axis of the SO without altering the dimension of the major axis.

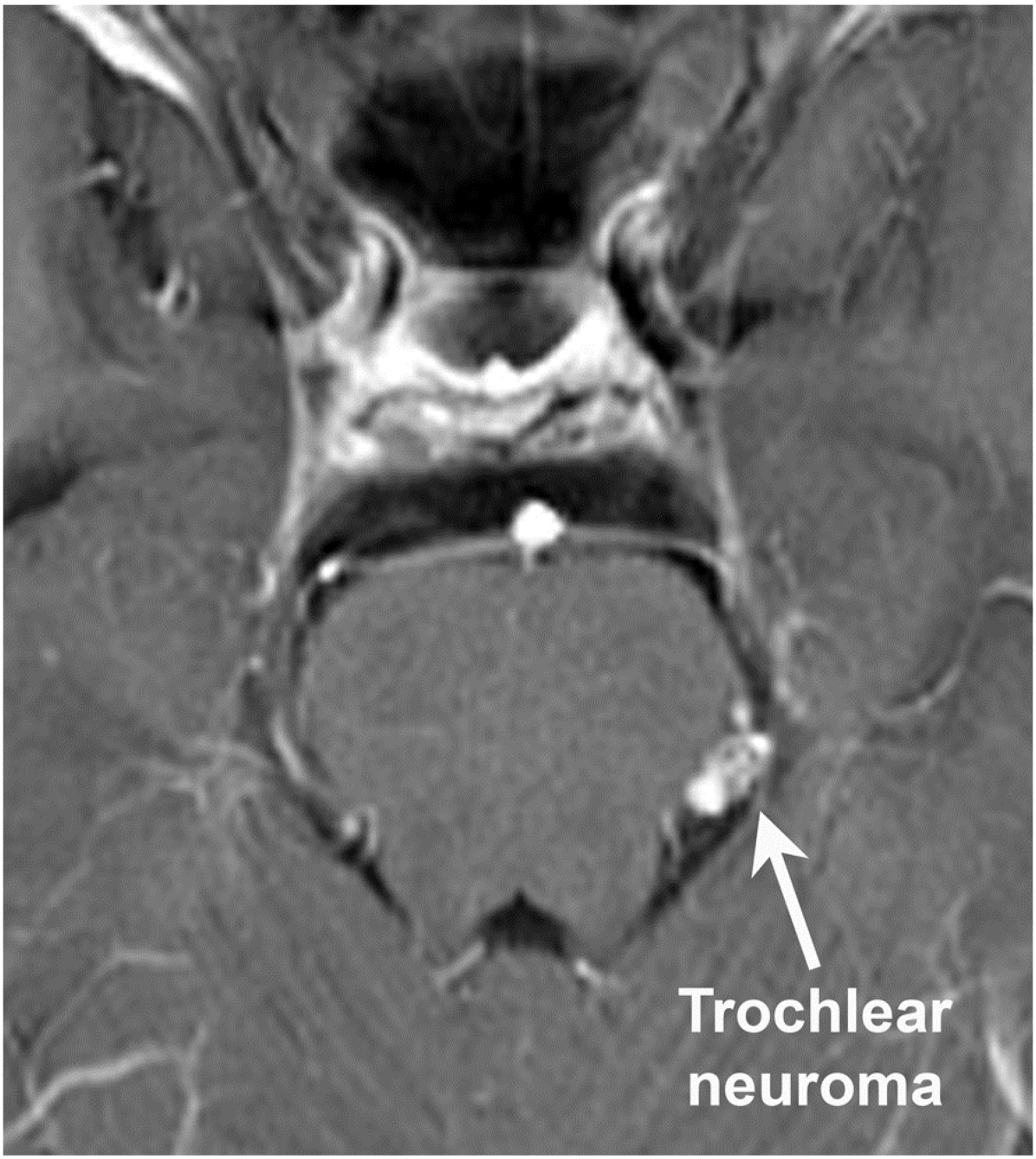

FIG 8.

Contrast T1 MRI demonstrating 5 mm enhancing nodule on the subarachnoid trochlear nerve in the left ambient cistern of case 8.

Table 1

Clinical and imaging findings in patients with schwannoma

Case	Age, years	Sex	Cranial nerve involved	Symptom duration, years	Initial negative imaging	Tumor location	Tumor size, mm	Shape
1	60	M	Medial rectus motor nerve	10	Yes	Deep orbit	2.9 × 3.9	Nodular
2	21	F	Medial rectus motor nerve	1	Yes	Deep orbit	3.3 × 2.8	Nodular
3	6	F	Medial rectus motor nerve	2	Yes	Deep orbit	4.7 × 7.7	Nodular
4	60	M	Oculomotor	20	No	Intracavernous and intraorbital	7.7 × 10 and 2.6 × 7.7	Fusiform
5	55	F	Oculomotor	5	Yes	Subarachnoid at posterior communicating artery	5 × 5	Nodular
6	60	M	Abducens	6	Yes	Subarachnoid	5 × 5	Nodular
7	45	M	Abducens	2	No	Subarachnoid and intracavernous	6 × 12	fusiform
8	50	M	Trochlear	5	Yes	Subarachnoid ambient cistern	5 × 5	Nodular